VDE VERLAG

IKMT 2015

Innovative Klein- und Mikroantriebstechnik

Innovative small drives and micro-motor systems

146

ETG-Fachbericht

Beiträge der
10. ETG/GMM-Fachtagung
14. – 15. September 2015
in Köln

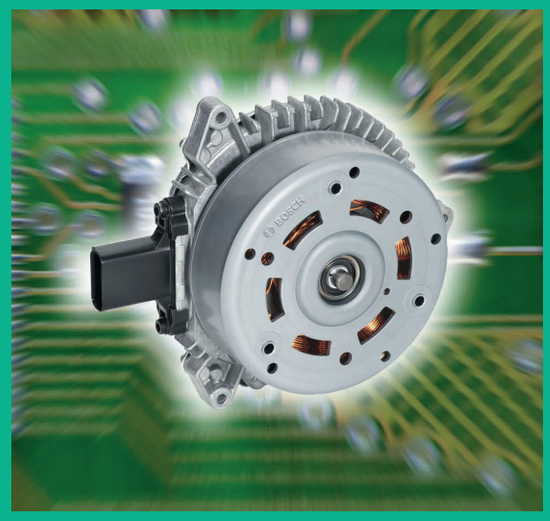

Energietechnische Gesellschaft im VDE (ETG)

Kontinuierliches Modell magnetischer Materialschädigungen durch Schnittflächeneinflüsse in der numerischen Simulation von Elektroblechen
Continuous model of magnetic material degradation due to cutting effects in the numerical simulation of electro laminations

S. Elfgen, S. Böhmer, S. Steentjes, D. Franck and K. Hameyer
Institute of Electrical Machines, RWTH Aachen University, Aachen, Germany
Email: silas.elfgen@iem.rwth-aachen.de

Kurzfassung

Die verschiedenen Verarbeitungsschritte in der Herstellung elektrischer Maschinen, wie beispielsweise Scherschneiden und Stanzen, beeinträchtigen die magnetischen Eigenschaften des weichmagnetischen Materials. Infolgedessen kann eine Abnahme der lokalen Permeabilität zusammen mit steigenden Hystereseverlusten in der Nähe der Schnittflächen beobachtet werden. Im Fall von geometrisch kleinen Maschinentopologien können Bereiche auftreten, in denen sich magnetische Schädigungen auch überlagern. Aktuelle Ansätze in numerischen Simulationen betrachten lokale Permeabilitätsveränderungen durch Unterteilung der schnittkantenbehafteten Bereiche eines Finite-Elemente (FE) Maschinenmodells in Gebiete unterschiedlicher Materialeigenschaften [1]. Mit diesem Ansatz ist jedoch die Abbildung eines kontinuierlichen Materialverhaltens innerhalb der Gebiete nicht möglich. Hieraus resultiert ein kompliziertes und aufwändiges Modell. Im Gegensatz dazu stellt dieser Beitrag ein kontinuierliches Modell zur Beschreibung der lokalen magnetischen Materialeigenschaften in der FE-Simulation vor. Es wird ein kristallographischer Ansatz gewählt. Als Ergebnis werden verbesserte Feld- und Verlustberechnungen erzielt.

Abstract

Different processing steps during the production of electrical machines, such as shear cutting and punching, adversely affect magnetic material properties. Therefore, a decreasing local permeability along with rising hysteresis losses in the vicinity of cut surfaces can be observed. Geometrically small machine topologies show significant overlap of magnetically damaged areas. Current approaches in numerical simulations consider permeability deteriorations by subdividing the iron parts of finite element (FE) machine models into slices of different material properties [1]. Using this approach a continuous material description across the slices is not possible. A complicated and effortful model arises. In contrast this paper presents a continuous model to reflect local magnetic material properties in FE-simulations. Therefore a cristallographic approach is chosen. As a result, improved field and loss calculations are achieved.

1 Introduction

The requirements on the properties of soft magnetic materials used for example in electrical machinery are increasing along with more efficient machine designs. In order to select the most appropriate material, it is characterised in terms of iron losses, saturation polarisation, permeability and frequency. Further the material behaviour due to manufacturing has to be considered. In particular small electric machines can suffer from cutting effects due to the smaller geometrical dimensions and their relatively longer total cutting length referred to the surface of the geometry. It is well known that fabrication steps, such as punching and shear cutting of magnetic material, lead to deterioration of its magnetic properties [2]. In case of shear cutting, plastic deformation and in case of laser cutting thermal stress is introduced to the material, leeding to residual stress inside the material [3, 4, 5]. As a consequence reduced average permeability caused by a changing local permeability distribution can be observed. Further effects are increasing hysteresis losses in the vicinity of cut surfaces, that lower the power density of the machine [6]. Particularly in case of small geometrically sized soft magnetic iron cores material deterioration can prevail [7, 8]. It is due to the fact, that areas of degraded permeability even interfere, depending on the manufacturing process and settings. This yields varying permeability distributions.

To cope with continuous, locally changing material properties attempts have been made to approximate them by subdividing the iron core of a model into slices of different magnetic material properties [1, 9, 10]. The different material properties are homogeneous across the corresponding slices. This approach lacks due to the constant material properties inside the subdivision in accuracy. Further,

in case of applications with non concentric transformable shapes as machines, a complicated modelling of slices arise during pre-processing. A more practical driven approach uses building factors to cope with a changed magnetisability and higher iron losses, but requires experience from the manufacturing process to estimate the resulting influences [11]. In light of these drawbacks, this paper presents a continuous material model, established in the numerical FE-simulation to describe local distributed magnetic material properties. It is based on the cristallographic model published in [12].

The paper is structured as follows. Section 2 briefly explains the sample set and its magnetic characterisation. Section 3 presents the continous material model, along with its implementation and parameter identification. Section 4 demonstrates the results of a FE-simulation using both the sliced and continuous model. The simulative results are then compared to measurements described in section 2. An exemplary stator tooth is simulated in order to underline the effect of locally varying magnetic material properties on the flux density distribution. Section 5 gives a discussion on the results along with an outlook for further studies.

2 Material samples and characterisation

Different attempts have been made with the aim to describe locally changing material properties starting with either measurements or analytical descriptions [1, 9, 13]. In case of measurements, at least two different attempts are common. One being magnetic measurements by e.g Single sheet measurements, inserting search coils, needle probes or dark field images [14, 13, 15], the other analysing the micro structural changes after a mechanical cut e.g. in terms of micro-hardness [8]. Consequently, mathematical models are developed that describe the measured permeability deterioration [16].

In order to identify the required model parameters in a single sheet tester (SST), describing the local magnetic material deterioration due to the cut surfaces, a set of single sheets of lamination is used. Starting with a basic sheet of 120 mm x 120 mm, **Figure** 1, samples with smaller width are consecutively cut out of the basic square. Thereby, single samples equalling a width b of 120 mm, 60 mm, 30 mm, 15 mm, 10 mm, 5 mm and 4 mm are produced. The material used for the sample set is M330-35A cutted by a CO2-Laser with a gas pressure of 10 bar, using a speed of 8 $\frac{\mathrm{m}}{\mathrm{min}}$ and a power of 1700 W.

In a next step the subdivided sheets are magnetically characterised using a SST. As a measuring sequence, a DC-hysteresis curve is measured. In order to measure the secondary voltage, a small time dependent flux density $\frac{dB}{dt}$ of 100 $\frac{\mathrm{mT}}{\mathrm{s}}$ is applied. The field strength values reach from 10 $\frac{\mathrm{A}}{\mathrm{m}}$ to 5000 $\frac{\mathrm{A}}{\mathrm{m}}$. Further hysteresis curves at a frequency of 50 Hz are measured. The measurements are performed using the field-metric method. All samples are measured with cutting directions parallel and perpendicular to the rolling

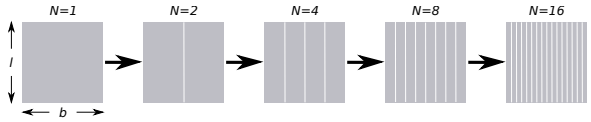

Figure 1 Structure of single sheet sample preparation.

direction. The results of the DC-measurement are shown in terms of magnetic polarisation and energy in **Figure** 2. For the data curves the results of the parallel and transversal direction are averaged. In the used case of a DC excitation only hysteresis losses are present. With a rising number of cuts applied to the specimens the hyperbolic loss curve converts into a nearly linear function.

In order to compare the results of FE-simulations to a measurable geometry, five toroidal cores are considered. The material and cutting parameters used, equal those of the measured single sheets, while the yoke diameter sizes are 15 mm, 7.5 mm, 5 mm, 3.75 mm and 2.5 mm. The iron core is stacked loosely and hold in shape using a Kapton tape and the wiring.

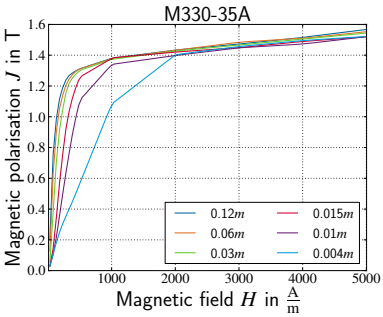

(a) Polarisation $J(H)$

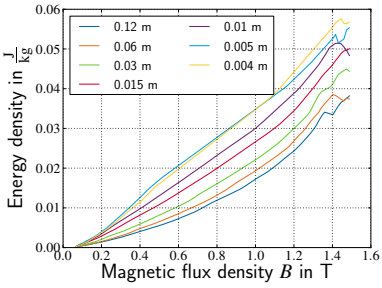

(b) Energy density $E(B)$

Figure 2 Results of the single sheet DC-measurements for different strip width averaged in parallel and transversal direction.

3 Continuous material modelling

In order to consider measured permeability deterioration in FE-simulations, FE-models are currently subdivided into slices of different permeabilities. These slices represent a coarse approximation of the continuous degradation profile [10, 1]. **Figure** 3 demonstrates the principles of a sliced model using the cross section of a toroidal core with a soft magnetic core surrounded by windings. The

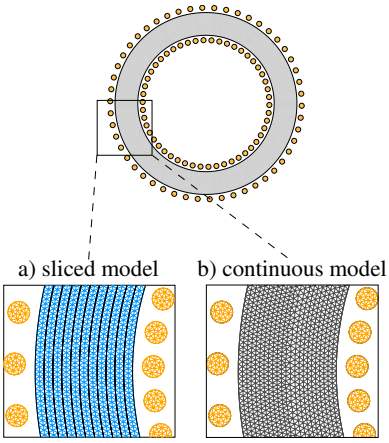

Figure 3 FE-mesh of a toroidal core model sliced into eleven strips a) and for continuous modelling b).

cut surfaces are placed at the inner and outer radius. On the left hand side the iron core is subdivided into slices of equal width. The material properties depend on the minimum distance to the cut surface. Consequently the material properties of the slices from the inner and outer radius are equal.

In view of an analytically solvable and symmetrical geometry, the modelling effort of a sliced model is simple. In contrary, when it comes to technically and physically relevant examples such as a rotating machine, the modelling effort is high[1]. Consequently a continuous material model which is independent of the used mesh is preferable and presented. Here three model parameters are needed to analytically describe the local magnetic polarisation dependent on the magnetic field H and distance to cut surface d. In contrary to [13], where model parameters depend on a certain specimen width, the continuous material model uses the distance to the cut surface as key parameter to describe the position specific permeability $\mu_r(x)$ in each location, independent of the current slice width b. With this approach it is possible to assign proper characteristic material curves to each element of the FE-mesh according to its distance to the cut surface. In the following the basic principles, the parameter identification and the adaptation made will be discussed.
The description of the local material behaviour in terms of a locally dependent relative permeability involves three parameters: the permeability of an undamaged material sample $\mu_r(H,N=0)$, the maximum permeability drop at the cut surface $\Delta\mu_{cut}(H)$, the function $\eta(x)$ describing the local deterioration shape. In contrary to other models, a description independent of the number of cuts N and the strip width b is achieved.

$$\mu_r(H,x) = \mu_r(H,N=0) - \Delta\mu_{cut}(H)\cdot\eta(x) \qquad (1)$$

The local deterioration profile $\eta(x)$ generally depends on the cutting method used. In case of mechanical cutting, hyperbolic profiles are reported [3, 4, 7, 13, 15]. In case of laser cutting profiles different profiles as well as non-symmetrical distributions are indicated in [15].

In the following, a parabolic permeability distribution is assumed described by $\eta(x)$:

$$\eta(x) = \left\{ \begin{array}{ll} 1-\frac{x}{\delta} - a\cdot\frac{x}{\delta}\left(1-\frac{x}{\delta}\right) & \text{for} \quad 0 \le x \le \delta \\ 0 & \text{for} \quad x > \delta \end{array} \right\} \qquad (2)$$

The model parameter δ indicates the depth of the area influenced by the cut surface, while the parameter a is a compression factor and x the distance to the cut edge. The maximum permeability drop at the cut surface is defined in [12] as the difference between the permeability of the undamaged specimen and a damaged one. The expression should be constant for all measured strip widths, which is achieved by scaling through a function value $F(N)$.

$$\Delta\mu_{\text{cut}}(H) = \frac{\mu_r(H,N=0) - \mu_r(H,N)}{F(N)} = \text{const}\ \forall\ b \qquad (3)$$

3.1 Parameter identification

The parameter identification is performed on basis of single sheet measurements using different strip width, as described in section 2. Considering the present and other material samples some adaptations are made in view of the parameter identification. In the process of parameter identification the best results are found when parameter a is assumed to be constant $a = 1$. As model parameter δ defines the depth of the mechanically influenced zone by the cut, local function $\eta(x)$ is only defined within the range of $x \le \delta$. In the following two variations of the damaged area are possible one being smaller than half of the strip width $\delta \le \frac{b}{2}$ the other a superposition in case of $\delta > \frac{b}{2}$. In [12] the limits of model parameter $\eta(x)$ were constrained by the quotient L/N, with L being the total width and N the number of cuts. As the restriction leads to an unsymmetrical polarisation distributions, it is replaced by $\frac{b}{2}$ as interval boundary.
The results of the parameter identification are depicted in **Figure** 4, comparing the modelled permeability to the measurements of specimens for different strip width. Measured and modelled data are generally in good agreement but reveal two areas for possible improvements. Firstly, a displacement of the measured maximum permeability, caused by superposing degenerated areas, with a rising number of cuts, can be observed for the present samples. Samples with small strip widths e.g. $b = 4\,\text{mm}$ loose the characteristic curve shape leading to an overestimated permeability. Secondly, the displacement between the maximum measured permeability and the exemplary permeability drop $\Delta\mu_{\text{cut}}$ results in degenerated material curves below $H = 100\,\frac{\text{A}}{\text{m}}$ especially in case of small widths.

3.2 Implementation of the material model in the FE-model

In order to use the continuous material model in FE-simulations an algorithm assigning each element a corresponding minimal distance to the cut surface is implemented. The distance of the element to the cutting edge is stored as additional property of the mesh element. As

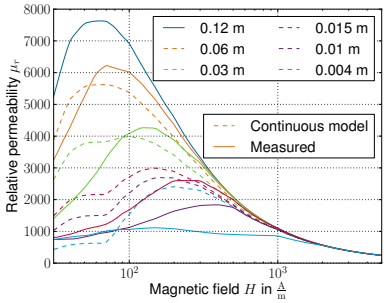

Figure 4 Comparison of the measured and modelled permeability.

the computational effort of handling a non-linear material curve for every element during simulation is too high, a material matrix is used. Here, a defined number of non-linear material curves, which correspond to a certain distance to the cut surface, are stored in matrix form. During simulation the distance of the current element is used to find the nearest entries inside the material matrix. An interpolation then calculates the material curves according to geometrical distances between the matrix entries.

4 Continuously modelled magnetisation behaviour

In order to compare simulation results of the two mentioned models and simulative results with measured data, different toroidal cores are used as listed in section 2. Utilising a geometry as testing object with a concentric moveable contour, a sliced FE-model is simple to build and a direct comparison to measured data is possible. Consequently iron loss calculations are performed in subsection 4.1.

To simulate the sliced model, each slice receives a particular material characteristic in terms of the magnetic reluctivity ν. The material characteristic in terms of magnetic permeability is calculated for each slice according to its distance to the cut surface. The distance value is set to the mean cut surface distance of the circular disc. In a next step, the material curves are calculated using the continuous material model. In case of the continuously simulated model only the element distance information and the material data matrix is needed. The excitation uses a current density as input parameter.

Exemplary results considering the flux density distribution inside the soft magnetic material at equal excitation, are shown in **Figure** 5. In the first case, Figure 5(a) the implemented continuous material model is depicted, in the second case, Figure 5(b) a sliced model with three slices and in Figure 5(c) an unaffected material curve is used. Two major aspects can be observed. Firstly the lower overall flux density and secondly the influence of the cut surface concentrating the flux to the centre of the toroidal core. As the permeability deterioration depends on the magnetic field strength, **Figure** 4, its effect is more pronounced at the outer radius.

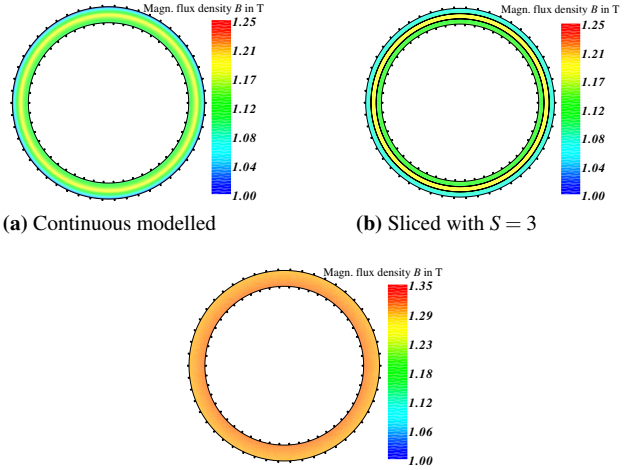

(a) Continuous modelled **(b)** Sliced with $S = 3$

(c) Without cutting effects

Figure 5 Resulting flux density of a toroidal core of 15 mm yoke width, using a continuously modelled material behaviour, a model with 3 slices and a characteristic material curve without cutting effects.

4.1 Iron loss calculations

In the following, iron loss calculations are shown comparing the simulation (sliced, continuous) with measured data. Quasi-static hysteresis losses are assumed to be the loss component, which is primarily affected by cutting [12]. Therefore quasi-static measurements on toroidal cores are performed as described in section 2. A simple linear approach is used with the parameters a_1 and α to describe the correlation between the flux density and the hysteresis losses.

$$P_{\text{hyst}} = a_1 \cdot B^{\alpha} \tag{4}$$

In view of material deterioration, rising hysteresis losses are related to cutting strains, which can be estimated by the proportion of the cut surface related to the remaining material area. Consequently parameter a_1 has to increase with smaller strip widths. Along with a rising number of cuts, a more linear behaviour of the Hysteresis losses can be observed, as shown in the measurement results Figure 2(b). To cope with the more linear behaviour, α has to decrease with smaller strip widths. A parameter identification is made to specify the hysteresis parameter $a_1(b)$ and $\alpha(b)$ dependent on the measured strip width using a least square fit method. The results of the identification for both the SST and toroidal core measurements are depicted in **Figure** 6(a) and **Figure** 6(b). The parameter a_1 identification of the SST is in good agreement with the measurement results of the toroidal cores. From the measurements and the parameter identification of a_1 can be concluded, that the cutting effect is more pronounced in parallel rolling direction as parameter a_1 doubles between the undamaged specimen of 120 mm and 4 mm. Further, with a rising number of cuts, an equalising effect of the anisotropy between the two directions can be observed, resulting in a nearly equal loss parameter a_1 for the smallest specimen.

With the identified parameter set hysteresis losses can be

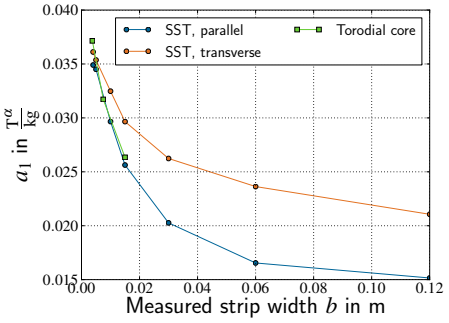

(a) $a_1(b)$

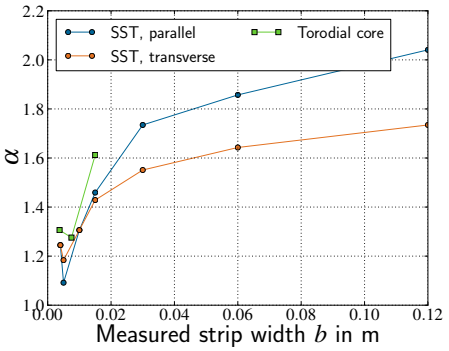

(b) $\alpha(b)$

Figure 6 Result of hysteresis loss parameter $a_1(b)$ and $\alpha(b)$ as a function of the measured strip width.

calculated using the results of the FE-simulations regarding the sliced and continuous model. Therefore a dependency on the strip width b is considered in the loss parameters. The losses are calculated by integrating over the local flux density solutions $B(x)$ defined modelled on the soft magnetic area Ω.

$$P_{\text{hyst}} = \int_{\Omega} \alpha_1(b) \cdot B(x)^{\alpha(b)} d\Omega \tag{5}$$

Exemplary results of the loss calculations are depicted in **Figure** 7. A comparison between three measured toroidal cores, the corresponding simulation of a model of three slices and the continuous model is shown. In order to graphically compare calculated and measured losses, the mean value of the FE-flux density solution is calculated. Regarding static hysteresis losses a good agreement between the simulation of both models and the measurements is achieved. Due to strongly damaged material the very small deviations between the sliced and continuous result. Simulative results of other materials which were e.g. cut by a guillotine obey a smaller influence depth and stronger deviations between a sliced and continuous model.

In **Figure** 8 a comparison of calculated and measured losses for a single toroidal core are shown. In case of an unaffected material sample (120 mm x 120 mm), used in the simulation, deviations arise with smaller flux density between the simulation and measurement. This underlines the importance of considering cut surface effects during simulation.

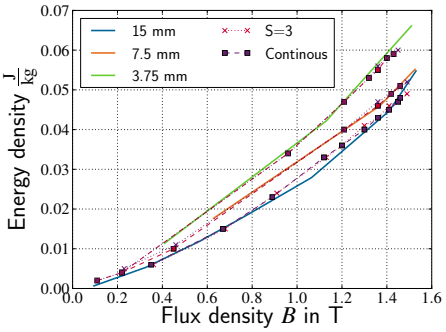

Figure 7 Comparison of the simulated model, using three slices $S = 3$ and the continuous model with measured energy losses for quasi-static excitation.

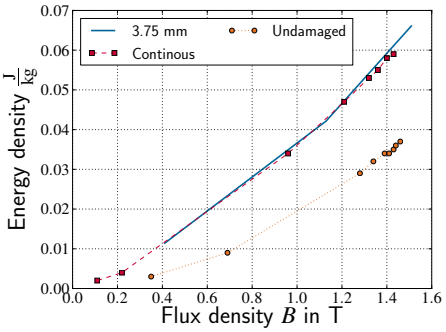

Figure 8 Comparison of the loss calculations using an undamaged material characteristic and the continuous model.

4.2 Application Example

The benefit of a continuously material model is evident on a technically relevant application. In order to briefly preview possible benefits of the continuous material model, the shape of a Stator tooth is shown in **Figure** 9. On the left side the flux density distribution resulting from a simulation using an undamaged material characteristic is depicted. In contrast, the continuously modelled solution is shown on right side. Even using this very simple structure, the basic cut surface effect on the flux density distribution can be demonstrated. Due to a reduced permeability at the surface a lower flux density results. Consequently, a flux concentration in the middle of the tooth can be observed. Along with the changed flux distribution changing local loss distribution arise which has to investigated further. In case of equal mean flux densities over the stator tooth, magnetic deterioration will lead to higher local flux density peaks resulting in increasing local magnetic and consequently thermal losses.

5 Conclusions

The deterioration of soft magnetic material due to cutting has been described by a continuous material model. Influences of the cut surface effect using a CO2-laser on toroidal cores with decreasing yoke width were measured. A continuous material model describing local permeability changes due to cut surface effects has been imple-

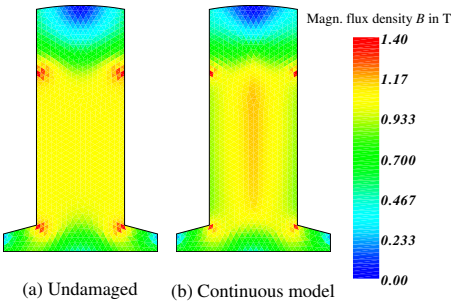

(a) Undamaged (b) Continuous model

Figure 9 Exemplary stator tooth with flux density distribution considering an undamaged and cut surface affected case.

mented and evaluated. A comparison was drawn in view of a sliced model considering flux density distribution and hysteresis losses. As a result, improved field calculations are achieved by continuously considering the changed flux distribution inside the damaged material, along with a reduced modelling effort. Furthermore, the impact of cut surfaces rises with smaller dimensions of the application. The model enables the simulation of rotating machines with a continuous local material deterioration and int the following improved local flux density distributions. Future work will concentrate on the degradation profile as well as on the superposition of residual stress to cope with the maximum displacement seen at the permeability characteristic curve.

6 References

[1] M. Bali, H. De Gersem, and A. Muetze, "Finite-element modeling of magnetic material degradation due to punching," *Magnetics, IEEE Transactions on*, vol. 50, no. 2, pp. 745–748, Feb 2014.

[2] A. Schoppa, J. Schneider, and C.-D. Wuppermann, "Influence of the manufacturing process on the magnetic properties of non-oriented electrical steels," *Journal of Magnetism and Magnetic Materials*, vol. 215–216, no. 0, pp. 74 – 78, 2000.

[3] V. Maurel, F. Ossart, and R. Billardon, "Residual stresses in punched laminations: Phenomenological analysis and influence on the magnetic behavior of electrical steels," *Journal of Applied Physics*, vol. 93, no. 10, pp. 7106–7108, 2003.

[4] G. Loisos and A. J. Moses, "Effect of mechanical and nd:yag laser cutting on magnetic flux distribution near the cut edge of non-oriented steels," *Journal of Materials Processing Technology*, vol. 161, no. 1–2, pp. 151 – 155, 2005, 3rd Japenese-Mediterranean Workshop on Applied Electromagnetic Engineering for Magnetic and Superconducting Materials and 3rd Workshop on Superconducting Flywheels.

[5] R. Siebert, J. Schneider, and E. Beyer, "Laser cutting and mechanical cutting of electrical steels and its effect on the magnetic properties," *IEEE*, vol. c2-09, pp. 1–4, 2008.

[6] K. Fujisaki, R. Hirayama, T. Kawachi, S. Satou, C. Kaidou, M. Yabumoto, and T. Kubota, "Motor core iron loss analysis evaluating shrink fitting and stamping by finite-element method," *IEEE Transactions on Magnetics*, vol. 43, no. 5, pp. 1950–1954, 2007.

[7] F. Ossart, E. Hug, O. Hubert, C. Buvat, and R. Billardon, "Effect of punching on electrical steels: Experimental and numerical coupled analysis," *Magnetics, IEEE Transactions on*, vol. 36, no. 5, pp. 3137–3140, Sep 2000.

[8] P. Baudouin, M. D. Wulf, L. Kestens, and Y. Houbaert, "The effect of the guillotine clearance on the magnetic properties of electrical steels," *Journal of Magnetism and Magnetic Materials*, vol. 256, no. 1–3, pp. 32 – 40, 2003.

[9] Z. Gmyrek and A. Cavagnino, "Analytical method for determining the damaged area width in magnetic materials due to punching process," in *IECON 2011 - 37th Annual Conference on IEEE Industrial Electronics Society*, Nov 2011, pp. 1764–1769.

[10] L. Vandenbossche, S. Jacobs, X. Jannot, M. McClelland, J. Saint-Michel, and E. Attrazic, "Iron loss modelling which includes the impact of punching, applied to high-efficiency induction machines," in *Electric Drives Production Conference (EDPC), 2013 3rd International*, Oct 2013, pp. 1–10.

[11] G. Müller, K. Vogt, and B. Ponick, *Berechnung elektrischer Maschinen*. Wiley-VCH, 2008, no. Bd. 2.

[12] L. Vandenbossche, S. Jacobs, F. Henrotte, and K. Hameyer, "Impact of cut edges in magnetization curves and iron losses in e-machines for automotive traction," in *Proceedings of 25th World Battery, Hybrid and Fuel Cell Electric Vehicle Symposium & Exhibition, EVS*, Schenzhen, China, November 2010.

[13] Schoppa and A.P., "Einfluss der be- und verarbeitung auf die magnetischen eigenschaften von schlussgeglühtem, nichtkornorientiertem elektroband," Ph.D. dissertation, RWTH Aachen, 2001.

[14] A. Moses, N. Derebasi, G. Loisos, and A. Schoppa, "Aspects of the cut-edge effect stress on the power loss and flux density distribution in electrical steel sheets," *Journal of Magnetism and Magnetic Materials*, vol. 215-216, pp. 690–692, 2000.

[15] R. Siebert, A. Wetzig, E. Beyer, B. Betz, C. Grunzweig, and E. Lehmann, "Localized investigation of magnetic bulk property deterioration of electrical steel: Analysing magnetic property drop thorough mechanical and laser cutting of electrical steel laminations using neutron grating interferometry," in *Electric Drives Production Conference (EDPC), 2013 3rd International*, Oct 2013, pp. 1–5.

[16] S. Steentjes, G. von Pfingsten, and K. Hameyer, "An Application-Oriented Approach for Consideration of Material Degradation Effects Due to Cutting on Iron Losses and Magnetizability," *IEEE Transactions on Magnetics*, vol. 50, no. 11, p. 7027804, November 2014.